



Citation for published version:

Díaz de Leon–Ortega, R, D'Arcy, DM, Lamprou, DA & Fotaki, N 2021, 'In vitro - in vivo relations for the parenteral liposomal formulation of Amphotericin B: A clinically relevant approach with PBPK modeling', *European Journal of Pharmaceutics and Biopharmaceutics*, vol. 159, pp. 177-187.
<https://doi.org/10.1016/j.ejpb.2020.03.001>

DOI:

[10.1016/j.ejpb.2020.03.001](https://doi.org/10.1016/j.ejpb.2020.03.001)

Publication date:

2021

Document Version

Peer reviewed version

[Link to publication](#)

Publisher Rights

CC BY-NC-ND

University of Bath

Alternative formats

If you require this document in an alternative format, please contact:
openaccess@bath.ac.uk

General rights

Copyright and moral rights for the publications made accessible in the public portal are retained by the authors and/or other copyright owners and it is a condition of accessing publications that users recognise and abide by the legal requirements associated with these rights.

Take down policy

If you believe that this document breaches copyright please contact us providing details, and we will remove access to the work immediately and investigate your claim.

1 *In vitro in vivo* relations for the parenteral liposomal formulation of Amphotericin B. Part 2: A
2 clinically relevant approach with PBPK modeling

3

4 R. Díaz de León–Ortega ¹, D. M. D'Arcy ², D.A. Lamprou³, N. Fotaki^{1,*}

5 ¹ Department of Pharmacy and Pharmacology, University of Bath, Bath, United Kingdom

6 ² School of Pharmacy and Pharmaceutical Sciences, Trinity College Dublin, Dublin 2, Ireland

7 ³ School of Pharmacy, Queen's University Belfast, Belfast, United Kingdom

8 * Corresponding Author

9

10 Dr Nikoletta Fotaki

11 Department of Pharmacy and Pharmacology

12 University of Bath

13 Claverton Down

14 Bath, BA2 7AY

15 United Kingdom

16 Tel. +44 1225 386728

17 Fax: +44 1225 386114

18 E-mail: n.fotaki@bath.ac.uk

19

20

21

22 **Abstract**

23 *In vitro* release testing is a useful tool for the quality control of controlled release parenteral
24 formulations, but *in vitro* release test conditions that reflect or are able to predict the *in vivo*
25 performance are advantageous. Therefore, it is important to investigate the factors that could
26 affect drug release from formulations and relate them to *in vivo* performance. In this study the
27 effect of media composition including albumin presence, type of buffer and hydrodynamics on
28 drug release were evaluated on a liposomal Amphotericin B formulation (Ambisome®). A
29 physiologically based pharmacokinetic (PBPK) model was developed using plasma
30 concentration profiles from healthy subjects, in order to investigate the impact of each variable
31 from the *in vitro* release tests on the prediction of the *in vivo* performance. It was found that
32 albumin presence was the most important factor for the release of Amphotericin B from
33 Ambisome®; both hydrodynamics setups, coupled with the PBPK model, had comparable
34 predictive ability for simulating *in vivo* plasma concentration profiles. The PBPK model was
35 extrapolated to a hypothetical hypoalbuminaemic population and the Amphotericin B plasma
36 concentration and its activity against fungal cells were simulated. Selected *in vitro* release tests
37 for these controlled release parenteral formulations were able to predict the *in vivo* AmB
38 exposure, and this PBPK driven approach to release test development could benefit
39 development of such formulations.

40

41 **Keywords:**

42 Amphotericin B; liposomes; PBPK; modeling; *in vitro*; release; PBPKPD; clinically; relevant

43

44

45 **1. Introduction**

46 A recent consensus document arising from a workshop dedicated to bringing consistency to
47 terminology used in dissolution testing has defined a clinically relevant *in vitro* release test as
48 the implication of a link between the *in vitro* release and the *in vivo* performance [1]. In order
49 to establish a clinically relevant test, it is important to understand how the test conditions (e.g.
50 media composition and hydrodynamics) affect the *in vitro* release from the formulation. In
51 some cases, the information obtained from *the in vitro* release tests is not enough to explain the
52 *in vivo* behaviour of the formulation and the released drug, and a mechanistic understanding of
53 the *in vivo* performance is required [2]. This can be achieved by the use of physiologically
54 based pharmacokinetic (PBPK) modeling. The general concept of PBPK modeling is to
55 mathematically describe relevant physiological, physicochemical, and biochemical processes
56 that determine the pharmacokinetic behaviour of a compound [3-5]. PBPK modeling and
57 simulation are currently a trending tendency and commercial software are available (for
58 example, Gastro- Plus[®], simCYP[®] or PK-Sim[®] [6]). PBPK modeling is now accepted by
59 regulatory agencies [7]. The Food and Drug Administration (FDA) have published the
60 “Physiologically Based Pharmacokinetic Analyses — Format and Content (Guidance for
61 Industry) [8]” and the European Medicines Agency (EMA) the “Guideline on the qualification
62 and reporting of physiologically based pharmacokinetic (PBPK) modelling and simulation
63 [9]”. A PBPK model can be developed considering 4 stages: i) setting the model equations to
64 represent the system, ii) input data to the model, iii) perform the simulation and iv) model
65 validation (observed vs simulated data, parameter sensitivity analysis) [2]. A sensitivity
66 analysis allows the identification of the parameters that have the greatest influence on the
67 simulation [10, 11].

68 A biopredictive release method consists of *in vitro* release testing conditions that, coupled with
69 mathematical modeling, are capable of predicting *in vivo* pharmacokinetic profiles [1]. PBPK

70 modeling can be extrapolated to simulate diseased populations, and could thus be used for
71 example for hypoalbuminaemic patients (plasma albumin < 25 g/L [12]), in order to investigate
72 the pharmacodynamics (PD) of the drug [13]. Hypoalbuminaemia can be observed in critically
73 ill patients with sepsis, who may be among the patient cohort administered AmB.

74 PBPK/PD models integrate the movement of the drug in the body with its pharmacological
75 activity [13]. In antimicrobial therapy, the pharmacological effect is the activity against an
76 infectious agent [14-16]. If a PBPK/PD model is used to evaluate the antimicrobial activity, for
77 many antimicrobial agents the microbial killing is considered to be dependent on the PK profile
78 of antimicrobial concentration in plasma [10, 17]. Amphotericin B (AmB) is a poorly soluble
79 highly protein bound drug used in the treatment of severe systemic fungal disease (e.g. *Candida*
80 *sp.*, *Aspergillus sp.* [18, 19]) and is commercially available as parenteral lipid formulations
81 (including the liposomal formulation Ambisome[®]) for intravenous administration. The
82 development of PBPK models for Amphotericin B in mice and rats after the administration of
83 Fungizone[®] (colloidal AmB) and Ambisome[®] have been reported [20, 21], which showed good
84 predictive performance after being extrapolated to humans. For PBPK modeling of
85 Ambisome[®], the uptake of particles by macrophage cells in organs like the liver and spleen,
86 were taken into account by using a saturable model. When this model was developed, the
87 authors reported that there was no *in vitro* AmB release data available and they determined a
88 value from fitting the model to the data with a release rate constant of 0.0035 h⁻¹ (in all the
89 tissues) with an initial rapid release of the 8% of the dose in humans [20, 21].

90 The aims of this study were i) to investigate how the presence of albumin in clinically relevant
91 media containing physiological surfactants (bile salts – phospholipids) [22]) combined with a
92 biorelevant hydrodynamic environment [23], impacts on the release of AmB from Ambisome[®];
93 ii) to develop a PBPK model to predict plasma drug concentrations in healthy subjects; iii)
94 coupled with the use of the PBPK model, to guide the development of a biopredictive *in vitro*

95 release test for the liposomal AmB formulation Ambisome[®]; iv) to extrapolate the PBPK model
96 to a hypoalbuminaemic population to build a PBPK/PD model to simulate the pharmacological
97 effect of AmB on fungal cells present in hypoalbuminaemic plasma vs plasma with normal
98 albumin levels.

99 **2. Materials and Methods**

100 **2.1. Materials**

101 AmB analytical standard (87.8%), methanol (MeOH) high performance liquid chromatography
102 (HPLC) grade, formic acid mass spectrometry grade, Sabouraud dextrose (SBD) broth, NaOH,
103 MgCl₂, CaCl₂, and NaHCO₃ were obtained from Sigma Aldrich (Germany); AmB API powder
104 (85%) from Cayman Chemical (USA); bovine serum albumin protease free powder fraction V
105 (BSA), dimethyl sulfoxide (DMSO), dextrose, sodium dodecyl sulphate (SLS), Na₂HPO₄,
106 NaH₂PO₄, KH₂PO₄, NaCl and KCl from Fisher Scientific (USA); phosphatidylcholine (PL)
107 from egg from Lipoid GmbH (Ludwigshafen, Germany); sodium taurocholate (BS) from
108 Prodotti Chimici e Alimentaria (Italy); Sabouraud dextrose (SBD) agar was obtained from
109 Oxoid (UK), 25 mL sterile universal culture tubes were obtained from Sterilin Thermo
110 Scientific (UK); 10 µL plastic loops from Microspec (UK); GF/D (pore size 2.7 µm, 25 mm
111 diameter) and GF/F (pore size 0.7 µm, 25 mm diameter) filters from Whatman (UK);
112 regenerated cellulose (RC) filters 0.45 µm 13 mm diameter from Cronus (UK); cellulose ester
113 dialysis tubing of 300 kDa MWCO from Spectrum Labs (USA), C18 Sep – Pak[®] Vac 3cc (500
114 mg) solid phase extraction (SPE) column from Waters (USA) and Ambisome[®] liposomal AmB
115 formulation from Gilead (Gilead, UK).

116 **2.2. Sample treatment of AmB in release media**

117 The sample treatment of AmB was described previously [23]. Briefly, the SPE method to
118 separate "liposomal AmB" (AmB still entrapped in the liposome) from "released AmB" (AmB

119 released from the liposome) was modified from Egger et al [24]. The SPE column was
120 conditioned with methanol, followed by water. 1.0 mL of sample was passed through the
121 column and the eluate was collected in a clean vial (liposomal AmB), the column was washed
122 with 2.0 mL of water and collected in the same tube. 1.0 mL of methanol was flushed through
123 the column to elute the AmB retained in the column (released AmB). In the case of samples
124 with proteins, proteins were precipitated by adding 2 volumes of methanol to 1 volume of the
125 sample followed by mixing in a vortex mixer, then centrifuged for 10 minutes at 12000 rpm
126 and 5°C. The supernatant was filtered through a 0.45 µm RC filter before injection to the
127 HPLC.

128 **2.3. Chromatographic conditions for the analysis of AmB from release media**

129 The chromatographic method to quantify AmB was described previously [25]. Briefly, AmB
130 was quantified by HPLC analysis using a Hewlett Packard Series 1100 equipped with an auto
131 sampler, temperature regulated column compartment, quaternary pump and diode array
132 detector (DAD detector) (Agilent Technologies). The column was a C18 Waters Sunfire
133 Column (Ireland) 150 x 46 mm 5 µm. The temperature of the column compartment was set at
134 25°C. The mobile phase consisted of formate buffer 50 mM pH = 3.2: MeOH (27.5:72.5, v/v);
135 the flow rate was 1 mL/min and analysis was performed with the DAD detector at $\lambda = 406$ nm.
136 The UV spectrum was recorded from 300 to 450 nm. Quantification of AmB in samples was
137 made based on calibration curves. Freshly prepared standard solutions (0.5 – 15 µg/mL) in the
138 corresponding medium were prepared by appropriate dilution of a 500 µg/mL stock solution
139 of AmB analytical standard in 1:1 MeOH: DMSO v/v. The limit of detection and the limit of
140 quantification were 0.12 and 0.37 µg/mL, respectively.

141 **2.4. *In vitro* release studies of AmB from Ambisome®**

142 The factors investigated for the development of the *in vitro* release studies were: i. the
143 composition of the clinically relevant media with biorelevant surfactants (media AmB
144 solubility value equivalent to that observed in plasma from healthy subjects [22]); media
145 composition factors explored were: type of buffer and BSA concentration, and ii. the
146 hydrodynamic conditions in terms of the apparatus used i.e. sample and separate (bottle/stirrer)
147 or continuous flow (flow through cell apparatus).

148 Media compositions were PBS BS 19.8 mM PL 7.9 mM and KRB BS 20.0 mM PL 4.0 mM,
149 with and without BSA 4.0% w/v. Media preparation was as previously described [22]. Briefly,
150 BS were weighed and dissolved in buffer and then PL from a stock solution of 100 mg/mL in
151 dichloromethane was added. Organic solvents were evaporated with a rotary evaporator set at
152 40°C and attached to a vacuum pump. The pressure was decreased from 650 mbar by steps of
153 70 mbar every two minutes to 100 mbar, where the pressure was maintained for 10 minutes.
154 When included in the medium, BSA was added after the evaporation of the organic solvents.

155 **2.4.1. Sample and separate method (bottle/stirrer setup)**

156 The sample and separate method was described previously [23]. Briefly, Ambisome® powder
157 (0.5 mg AmB) was placed into a 100 mL glass bottle with 30 mL of release medium and stirred
158 with a magnetic stirrer at 37°C. Release studies were performed based on a two-level factorial
159 design of experiments (DoE). The factors investigated (composition of release media and
160 agitation conditions) are shown in Table 1; the combination of all the factors resulted in eight
161 experimental setups.

162 The agitation rates in the bottle/stirrer setup were selected based on the linear velocity of the
163 stirrer edge, which at 130 rpm (10.2 cm/s) is comparable to the linear flow velocities in
164 vein/arteries and at 380 rpm (29.5 cm/s) to flow velocities in the aorta [23]. Sampling times
165 were 1, 2, 4, 6, 8, and 12 h and after sample treatment (SPE and protein precipitation), samples

166 were injected to the HPLC and AmB concentration in the samples was determined. All
167 experiments were performed in triplicate.

168 **2.4.2. Continuous flow (flow through cell apparatus)**

169 The flow-through apparatus setup was described previously [23]. Briefly, AmB release studies
170 were carried out in a flow-through dissolution apparatus (Sotax CE7 smart connected to a Sotax
171 piston pump CP7, Sotax, Aesch Switzerland) operated in the closed mode [26]. A 5 mm ruby
172 glass bead was positioned at the bottom of the cell (large cell: 22.6 mm diameter). The dialysis
173 membrane was placed into the flow through cell apparatus dialysis adapter and Ambisome[®]
174 powder (0.5 mg AmB) was placed into the membrane with 1 mL of the release medium. Glass
175 fibre filters (GF/D, GF/F) were positioned at the top of the cell. The release studies were based
176 on a two level factorial DoE, where the velocities used were considered biorelevant: “Low
177 velocity” (flow rate: 8 mL/min) has an average linear velocity comparable to capillary flow
178 and “High velocity” (flow rate: 35 mL/min) is comparable to intermediate capillary-vein flow
179 [23] and BSA presence (4.0% w/v) or not were the factors investigated. 36 mL of KRB BS
180 20.0 mM PL 4.0 mM (with or without BSA) were used in order to simulate the equivalent
181 volume available on administration of 1 mg/kg of AmB as Amphotericin B[®] to a 70 kg subject
182 (assuming 5 L of blood volume). Furthermore, as the 36 mL volume used does not allow for
183 distribution as would happen *in vivo*, it represents an extreme case in terms of available volume.

184

185 **2.5. Release data treatment**

186 The release data treatment was described previously [23]. Briefly, for the studies with the
187 sample and separate method, % AmB released over time was calculated based on the % AmB
188 still entrapped in the liposomes at the time of sampling ($\%AmB_{liposomal}$) (Eq 1) to construct

189 the calculated $\%AmB_{released}$ profile. $\%AmB_{released} = \%AmB_{initial} - \%AmB_{liposomal}$

190 (Eq 1)

191 where $\%AmB_{initial}$ is the mass of AmB placed into the reservoir initially (100%) and

192 $\%AmB_{released}$ is the calculated AmB percent released.

193 For the studies with the continuous flow setup the $\%AmB_{released(obs)}$ over time was corrected

194 for degradation using Eq 2 to construct the calculated $\%AmB_{released}$ profile.

195 $\%AmB_{released} = \%AmB_{released(obs)} + k_{deg} * AUC_{0-t}$ (Eq 2)

196 where $\%AmB_{released}$ is the corrected % AmB released accounting for degradation,

197 $\%AmB_{released(obs)}$ is the % AmB released at time t , AUC_{0-t} is the Area Under the Curve of

198 the observed concentration – time curve from time 0 to time t and k_{deg} is the degradation rate

199 constant obtained from the degradation experiments [22].

200 The AmB release rate constant (k_{rel}) from Ambisome[®] was obtained from first order fitting

201 of calculated $\%AmB_{released}$ individual profiles (Equation 3) and mean and standard deviation

202 values were calculated (GraphPad Prism 7, GraphPad Software, Inc, USA).

203 $\%AmB_{released} = \%AmB_{releasedmax} * (1 - e^{-k_{rel}t})$ (Equation 3),

204 where $\%AmB_{releasedmax}$ is the maximum AmB percent released and t is time.

205 **2.6. Atomic Force Microscopy (AFM) studies**

206 To further investigate the effect of the clinically relevant media components (e.g. BS, PL and

207 BSA) on the liposomes, AFM studies were performed. The AFM methodology has been

208 described previously [23]. Ambisome[®] liposomes were incubated in KRB BS 20.0 mM PL 4.0

209 mM BSA 4.0% w/v (for 30 min) and in KRB BS 20.0mM PL 4.0 mM (for 5 min; a shorter

210 period of incubation was set in order to reflect the fast release of AmB from the liposomes

211 observed in the absence of BSA). After the incubation time, samples were centrifuged for 30
212 min at 13,300 rpm in an Eppendorf centrifuge, the supernatant was discarded and the pellet
213 was dried under vacuum. The pellets were diluted with 1 mL of HPLC water, and then 10 μ L
214 of the liposomal solution was placed on a freshly cleaved mica surface (1.5 cm \times 1.5 cm; G250-
215 2 Mica sheets 1" \times 1" \times 0.006"; Agar Scientific Ltd., Essex, UK). The sample was then air-
216 dried for \sim 30 min and imaged immediately by scanning the mica surface in air under ambient
217 conditions using a Bruker MultiMode 8 Scanning Probe Microscope (Bruker, Billerica,
218 Massachusetts, USA) operated on Peak Force QNM mode. The AFM measurements were
219 obtained using ScanAsyst-air probes (Bruker, Billerica, Massachusetts, US); the spring
220 constant was calibrated by thermal tune (Nominal 0.4 N m⁻¹) and the deflection sensitivity
221 calibrated using a silica wafer. AFM scans were acquired at a resolution of 512 \times 512 pixels at
222 scan rate of 1 Hz, and produced topographic images of the samples in which the brightness of
223 features increases as a function of height. The raw image data were processed using Bruker
224 Nanoscope Analysis (version 1.5), and height images were flattened to remove sample tilt and
225 scanner bow. The surface roughness (R_a) of each substrate was determined by using Nanoscope
226 Analysis' algorithm to analyse several scans of the surface from different locations (n = 20).
227 AFM images were collected from random spot surface sampling (at least four areas).

228 **2.7. PBPK modeling for Ambisome[®] administration to healthy subjects**

229 **2.7.1 Data for PBPK modeling.**

230 Published data of plasma concentration profiles from a population of 5 healthy subjects (4
231 males, 1 female; ages from 33 to 65 years; height from 1.61 to 1.68 m; and weight from 68 to
232 86 kg) administered 2.0 mg/kg of Ambisome[®] by intravenous infusion over 2 h where the
233 "liposomal AmB" and "released AmB" were quantified [27, 28], were digitalized with Webplot

234 digitalizer 3.8 software. "Liposomal AmB" and "released AmB" distribution, clearance, protein
235 binding and physicochemical properties are shown in Table 2.

236 The PK parameters (distribution, clearance and protein binding) for "released AmB" were as
237 reported by Kagan et al. after administration of the colloidal AmB formulation Fungizone®
238 [21] (Table 2). Protein binding was characterized by k_{diss} (equilibrium dissociation constant).
239 The nominal glomerular filtration rate (GFR) for AmB was 0.08 mL/min/kg as calculated using
240 Eq 4, based on a fraction unbound of 0.05. This value was used to calculate the GFR fraction
241 for the "liposomal AmB" and "released AmB".

$$242 \text{ Nominal GFR} = \text{fraction unbound (albumin)} * (120 \text{ mL/min}) * (1/73 \text{ kg}) \quad \text{Eq}$$

243 4.

244 The biliary elimination rate constant was calculated using Eq 5.

$$245 k_{bil} = (Cl_{biliary}/\text{distributuion volume})(60 \text{ min}/1 \text{ h}) \text{ Eq 5.}$$

246 For the development of the model, "liposomal AmB" was assumed to behave as a molecule as
247 the concentration of AmB is what is quantified in the *in vivo* studies and not the concentration
248 or amount of liposomes.

249 An "immune" enzyme was added for the "liposomal AmB" to account for the removal of
250 circulation of the "liposomal AmB" by the macrophages of the immune system. The enzyme
251 was set to be located in the plasma, liver and spleen. The fraction unbound value for the
252 "liposomal AmB" was hypothesized to be smaller than 0.95 based on the reported interaction
253 between albumin and liposomes [38-40]. All the other parameters were left as software default
254 values.

255 **2.7.2. Workflow for PBPK modeling of Ambisome®**

256 The workflow for the PBPK modeling to describe the pharmacokinetics of "liposomal AmB"
257 and "released AmB" in a healthy individual after the administration of the Ambisome[®] is
258 presented in Figure 1.

259 PBPK modeling was performed with PKSim[®] 7.2.1 (Bayer, Germany) and MoBi[®] 7.2 (Bayer,
260 Germany). The five parameters listed in Figure 1 were optimized simultaneously with the
261 MoBi[®] built in function "Parameter identification" using an algorithm based on Monte Carlo
262 methods and the default software setup (the Parameter identification tool varies selected input
263 parameters in a given range to identify the best values to obtain output simulated curves similar
264 to the observed curves). The *in vivo* release of AmB from the liposomes was set to occur only
265 in plasma (k_{rel-iv}).

266 Comparing the developed PBPK model in this study with that reported by Kagan et al [21],
267 there were some differences: i) this model was developed in order to link the *in vitro* release
268 data to the observed plasma concentration data while Kagan and co-workers developed their
269 model to have a better understanding of AmB PK in order to improve dosing; ii) the model
270 developed by Kagan et al. assumed that release of AmB took place in all compartments [21]
271 while in this study, the release was modelled in plasma only.

272 Sensitivity analysis was performed on all the parameters of the model (PK parameter estimates
273 and physicochemical properties of "liposomal AmB" and "released AmB") except for the
274 molecular weight and the pKa values of "released AmB". The parameters and the range in
275 which the sensitivity analysis was evaluated are presented in Table 3.

276 The ranges were selected as follows: logP of "liposomal AmB" and "released AmB": ± 1 log
277 unit of the optimized value, immune enzyme of "liposomal AmB": ± 1 h⁻¹ of the optimized
278 value, aqueous solubility of "released AmB": the range was selected to cover the solubility
279 values reported in the literature [33-35], aqueous solubility of "liposomal AmB": ± 200 $\mu\text{g/mL}$

280 in order to cover a wide range as the solubility value was calculated by considering the total
281 amount of formulation powder in a vial (14.5 g), dissolved in 50 mL of water (Table 2); for
282 radius solute ("liposomal AmB"), biliary clearance ("liposomal AmB" and "released AmB"),
283 k_{diss} of lipoprotein B (APOB) and alpha1-acid glycoprotein (AAG1) the interval was $\pm 50\%$
284 of the literature value (Table 2 and 3). The GFR fraction ("liposomal AmB" and "released
285 AmB") was investigated ranging from 0 to 1; and the unbound to protein fraction ("liposomal
286 AmB" and "released AmB") from 0.05 to 0.95. k_{rel-iv} was investigated in the interval of the
287 k_{rel} found in the *in vitro* tests (Table 3). AUC_{0-24h} of both liposomal and released AmB was
288 used as response to evaluate the effect of the parameters investigated. Sensitivity analysis was
289 performed with the MoBi Toolbox for R esqLABS version 7.2.1 (esq LABS, Germany). All
290 the intervals tested, were normalized to 0 – 1 for clarity of presentation.

291 After the sensitivity analysis, the model was applied to the population described in section
292 2.7.1. The variability (standard deviation) for the parameters input into the model was as
293 described in Table 2. As the values of k_{rel-iv} and specific clearance for the immune removal
294 "enzyme" were obtained by parameter identification and there are no reported values for their
295 variability, 20% of the identified value was used as standard deviation.

296 **2.7.3. Evaluation of the *in vitro* tests using PBPK modeling**

297 The *in vitro* k_{rel} (Mean \pm SD) obtained from the *in vitro* release profiles of AmB from
298 Ambisome[®] were input to the validated PBPK model in order to predict the observed *in vivo*
299 AmB ("liposomal AmB" and "released AmB") plasma concentration profiles. The AUC_{0-24h}
300 was calculated from the predicted "liposomal AmB" and "released AmB" plasma concentration
301 profiles.

302 **2.8. PBPK-PD model for the pharmacological activity of AmB against *Candida albicans***

303 The effect of AmB on *Candida albicans* (*C. albicans*) was investigated in order to develop a
304 PBPK-PD model: i. for a patient population receiving Ambisome® with a reduced albumin
305 plasma concentration (hypalbuminaemia: albumin < 25 mg/mL), and ii. for a healthy
306 population receiving Ambisome® with normal concentration of albumin (~4.0% w/v).

307 **2.8.1. Quantification of *C. albicans***

308 The culture and quantification of *C. albicans* was described previously [25]. A single colony
309 culture was started in a tube with 5 mL of SBD broth and incubated overnight at 37°C in a
310 shaking incubator; the optical density was measured at 600 nm (OD₆₀₀). The colony forming
311 units (CFU) were determined by preparing serial dilutions and the suspensions were plated on
312 SBD agar plates, incubated overnight at 37°C and the number of colonies were counted and
313 related to the OD₆₀₀ of the culture.

314 **2.8.2. Time killing experiments**

315 Time killing experiments were performed with 10⁵ CFU/mL of *C. albicans* using different
316 AmB final concentrations (0.00, 0.75, 1.50 and 3.00 µg/mL) in the presence of BSA 2.0% and
317 4.0% w/v in KRB [an experiment without AmB was performed in order to obtain the k_{growth}
318 of the fungal cells]. The % CFUs remaining at each time point were used for curve fitting to
319 the exponential decay equation to obtain the killing rate coefficient for each concentration
320 tested (Eq 6).

$$321 \%CFU = \%CFU_{max} * e^{-k_{kill}t} \text{ Eq 6.}$$

322 where %CFU is the %CFU at time t , %CFU_{max} is the maximum %CFU, k_{kill} is the time killing
323 rate coefficient and t is time.

324 A linear relation was found between k_{kill} and AmB concentration and it was used in the PBPK-
325 PD model.

326 **2.8.3 PBPK-PD modeling**

327 The workflow for the development of the PBPK-PD model is shown in Figure 2.

328 To simulate a hypoalbuminaemic patient population, the protein content was halved in the
329 validated PBPK model for the healthy subjects and the rest of the parameters remained
330 unchanged. The "released AmB" concentration was used to calculate the k_{kill} for the 24 h time
331 course to simulate the "released AmB" activity against *C. albicans* which was set at a
332 concentration of 10^5 CFU/mL at time zero. The *C. albicans* growth rate constant (k_{growth}) was
333 obtained from the control time killing experiment (0.00 µg/mL AmB) by fitting the data to an
334 exponential growth equation (Eq 7)

$$335 \%CFU = Ae^{k_{growth}t} \text{ (Eq 7)}$$

336 where %CFU is the %CFU at time t, A is the starting CFU value, k_{growth} is the growth rate
337 constant and t is time.

338 **2.9. Statistical analysis**

339 The statistical analysis was described previously [23]. Pareto charts, based on the DoE analysis,
340 were performed for the identification of significant effects from the *in vitro* release tests. A
341 factor was significant when the standardized effect (bars) was larger than the line for statistical
342 significance level ($\alpha = 0.05$) (vertical line). An independent means t – test was performed to
343 compare 2 independent means: in the AFM studies, size and surface roughness were compared
344 against the control sample. A $p < 0.05$ was considered statistically significant. Due to the lack
345 of individual observed data of plasma concentration profiles, the *in vitro* k_{rel} were input into
346 the PBPK model to obtain simulated AUC_{0-24h} which were compared against the AUC_{0-24h}
347 obtained from the simulated data generated by the validated PBPK model.

348 Additionally, the 90% confidence interval (90% CI) for the ratio of the geometric means of the
349 simulated AUC_{0-24h} obtained with the *in vitro* k_{rel} and the AUC_{0-24h} obtained from the
350 simulated data generated by the validated PBPK model were calculated. As recommended by
351 the FDA guidance, both "liposomal AmB" and "released AmB" were evaluated [39]. Data
352 analysis, creation and analysis of DoE were performed with the statistical software Statgraphics
353 Centurion XVII (USA) and the 90% CI were calculated with IBM SPSS Statistics 25 (USA).

354 **3. Results and discussion**

355 **3.1. *In vitro* release testing of Ambisome®**

356 *In vitro* release profiles of AmB from Ambisome® in both hydrodynamic setups are shown in
357 Figure 3 and parameters obtained after fitting to the first order equation model are presented in
358 Table 4.

359 For the sample and separate setup, the statistical analysis (Figure 4a) showed that the buffer
360 was a significant factor affecting $\%AmB_{released}max$ with a higher release in KRB, the
361 presence of BSA 4.0% w/v had a significant negative effect. The interaction between buffer
362 and BSA was significant as the amount released in KRB with BSA is slightly higher than in
363 PBS with BSA, while in media without BSA there is no difference. The release rate constant
364 was affected in the same way as $\%AmB_{released}max$ but the interaction between buffer and
365 BSA showed that the release rate is faster in KRB than in PBS without BSA and there is not a
366 statistical significant difference in KRB and PBS with BSA. For the continuous flow setup
367 (Figure 4b), the flow rate was the only significant factor affecting AmB release from the
368 liposomes, with a positive effect on the AUC_{0-12h} .

369 **3.2. AFM studies**

370 Figure 5 shows the images obtained from the AFM and Table 5 contains the parameters of the
371 liposome characteristics measured by AFM.

372 Diameter of the liposomal structures in samples from KRB BS 20.0 mM PL 4.0 mM are
373 significantly higher than the control sample; liposomes could be merging with each other or
374 the inclusion of BS PL could alter the structure of the liposome resulting in a higher size before
375 the disruption. Liposomes were not visible in the sample of from KRB BS 20.0 mM PL 4.0
376 mM BSA 4.0% w/v, probably due to the incubation period of this sample.

377 **3.3. PBPK modeling of Ambisome[®] administered to healthy subjects**

378 The simulated plasma concentration profiles obtained with the validated PBPK model for the
379 administration of Ambisome[®] to healthy subjects are shown in Figure 6.

380 Using the parameter identification method, the optimal values for the parameters investigated
381 were: $k_{rel-iv} = 0.60 \text{ h}^{-1}$, $\log P$ (released AmB) = 3.24, $\log P$ (liposomal AmB) = 1.0, Specific
382 clearance for the immune removal "enzyme" = 2.57 h^{-1} and AAG1 $k_{diss} = 0.42 \text{ } \mu\text{mol/L}$. The
383 $\log P$ and $\text{clog} P$ values reported in the literature, are between -2.33 to 2.14 (Table 2) providing
384 a wide interval for the true value. The value obtained from parameter identification fitting was
385 3.24 which could be supported considering the distribution of the values previously reported
386 (Table 2).

387 The PBPK model described closely the average observed data for "liposomal AmB" and
388 "released AmB" ($\% .AUC_{0-24h} \text{ predicted} / AUC_{0-24h} \text{ observed}$ were 94% and 101%,
389 respectively). Comparing the developed PBPK model in this study with the one reported by
390 Kagan et al [21], the main difference was the k_{rel-iv} from this model was faster: $0.60 \text{ h}^{-1} >$
391 0.0035 h^{-1} [21] and there was no initial rapid release of 8.0% of the dose, as was included by
392 Kagan et al [21]. It could be due to simulated AmB release taking place in all of the

393 compartments in the model presented by Kagan et al. [21], while in this study; the release was
394 only in plasma.

395 The sensitivity analysis is shown in Figure 7. Parameters such as aqueous solubility ("liposomal
396 AmB" and "released AmB"), solute radius ("liposomal AmB"), specific biliary clearance
397 ("liposomal AmB" and "released AmB"), k_{diss} for AAG1 and APOB ("released AmB"), and
398 the GFR for "released AmB" did not have a significant impact on the AUC_{0-24h} of "liposomal
399 AmB" or "released AmB". For the "liposomal AmB", the fraction unbound to proteins had the
400 greatest impact on the model. It can be observed how the "liposomal AmB" in plasma decreases
401 as the fraction unbound increases, leading to a decrease in "released AmB", as there will be
402 less "liposomal AmB" available in plasma to release drug. k_{rel-iv} had a high impact on both
403 "liposomal AmB" and "released AmB" (Figure 7), with a higher release rate constant leading
404 to an increase in the "released AmB" and a decrease in the "liposomal AmB". For "released
405 AmB", logP is the factor with the highest effect on AUC_{0-24h} .

406 **3.4. Evaluation of the *in vitro* release profiles using the PBPK model**

407 The predictability of the *in vitro* release tests is presented in Figure 8 for both "liposomal AmB"
408 and "released AmB".

409 For the "liposomal AmB", the AUC_{0-24h} obtained with the *in vitro* k_{rel} where BSA was present
410 in the media were similar to the AUC_{0-24h} obtained from the validated PBPK model, regardless
411 of the type of the buffer or the hydrodynamic conditions. The AUC_{0-24h} values were only
412 similar for a medium without BSA in the low velocity setup (Figure 8). For the "released
413 AmB", the AUC_{0-24h} obtained with the *in vitro* k_{rel} in media with BSA were close to attaining
414 similarity to the *in vivo* profiles, as all the tests (except KRB BS PL BSA low agitation)
415 revealed one extreme of the 90% CI between 80 – 125%. It can be noticed that the tests
416 performed with the continuous flow setup under-predicted the plasma concentration of the

417 "released AmB". An increasing flow rate leads to a higher drug release (Figure 4) thus further
418 exploration of flow rate effect could be conducted to identify the flow rate resulting in release
419 profiles suitable for simulation of *in vivo* release. The AUC_{0-24h} could not be calculated for
420 the high velocity profiles as for the medium without BSA the standard deviation was higher
421 than the mean and for the medium with BSA the profiles could not be fitted to the first order
422 equation. The model developed is suitable for the evaluation of the *in vitro* release tests and
423 could support the development of a biopredictive *in vitro* release test. It has to be noted that for
424 the prediction of the plasma concentration of "liposomal AmB" and "released AmB", the
425 presence of BSA was a critical factor, thus, information on the exact mechanism of the protein
426 binding to the liposomes could further improve the model developed. Furthermore, the
427 accuracy of model could be further improved through inclusion of parameters capturing AmB
428 binding to red blood cells, as in general only plasma concentrations are presented in the
429 literature while the formulation is obviously administered to the venous blood pool.

430 **3.5. PBPK – PD modeling for the patient (hypoalbuminaemic) population.**

431 Parameters obtained after fitting to the exponential decay equation model for the time killing
432 experiments are presented in Table 6. A linear relationship between the AmB concentration
433 and the time killing rate coefficient was found for experiments with BSA 2.0 and 4.0% w/v,
434 (Eq 8 and eq. 9, respectively)

$$435 \text{ time killing rate coefficient } (h^{-1}) = 0.1923(mL * h^{-1}) / \mu g + 0.2102 h^{-1} \text{ Eq 8.}$$

$$436 \text{ time killing rate coefficient } (h^{-1}) = 0.1167 (mL * h^{-1}) / \mu g + 0.014 h^{-1} \text{ Eq 9.}$$

437 The simulated plasma concentration profiles for "liposomal AmB" and "released AmB" in the
438 extrapolated hypoalbuminaemic population and the healthy subject population are presented in
439 Figure 9a. It can be observed that both "liposomal AmB" and "released AmB" are at a lower
440 concentration as a consequence of the decrease of the amount of proteins present. There is a

441 lower concentration as with more unbound drug there is more drug available for distribution
442 and clearance. Figure 9b shows the simulated plasma concentration profiles for a typical
443 administration of Ambisome[®] to a patient with a systemic fungal infection (300 mg, infusion
444 4 h) in the simulated hypoalbuminaemic patient and in a subject with normal albumin levels.

445 Equations 8 and 9 were used in the PBPK-PD model to simulate the killing of *C. albicans*
446 (Figure 9c). It can be observed how the growth of the fungal cells is reduced by the
447 administration of Ambisome[®] (Figure 9d) with a higher effect in the simulated
448 hypoalbuminaemic patient than in the subject with normal albumin levels. From the time
449 killing studies and previous data on minimum inhibitory and fungicidal concentrations [25], a
450 higher fungicidal effect is reached with a lower AmB concentration in the presence of BSA
451 2.0% w/v as there is more unbound drug able to exert its pharmacological effect. It has to be
452 noted that only the effect of released AmB is evaluated in this PBPK-PD model. The humoral
453 and cellular immune responses and the effect that the liposomal AmB could have on *C.*
454 *albicans* are not considered, nor is the effect of fungal phospholipases on liposomal integrity
455 and AmB release. A number of 10⁵ CFU/mL were used to simulate the effect of AmB *in vivo*
456 as this was the concentration of the fungal cell suspensions used in the time killing experiments.

457 It has been reported that a concentration of 100 – 1000 CFU/mL are found in cultures of blood
458 from patients with systemic fungal infection [41, 42]. The PBPK-PD analysis could be further
459 improved by using the adequate number of CFU quantified in plasma from infected patients to
460 evaluate the response of the humoral immune response and not only the effect of the protein
461 content. In plasma from healthy subjects the fungal cells did not grow (data not shown), thus,
462 the results of the PBPK-PD model for the healthy subject must be only considered as an
463 exercise for comparative purposes. For this model, only the changes in the albumin levels were
464 considered, leaving aside the physiological characteristics of septic or critically ill patients. In
465 order to improve the model, the change in the activity of the immune enzyme should be

466 adjusted to the patient population as the immune system might be compromised or activated,
467 and the k_{rel-iv} , which the *in vitro* tests showed to be dependent on the albumin concentration,
468 should also be adjusted. This approach reveals the potential of the use of *in vitro* release data
469 and suitable microbiology data in combination with a PBPK-PD model in order to guide
470 parenteral formulation development based on pharmacodynamics and therapeutic outcomes.

471 **4. Conclusions**

472 The literature available for *in vitro* release testing of controlled release parenteral formulations
473 is limited. The evaluation of factors that can affect the release from these formulations and the
474 development of *in vitro* release tests that are able to predict the *in vivo* performance are of high
475 importance. In this work, the development of a clinically relevant *in vitro* release test for the
476 liposomal formulation of AmB (Ambisome[®]) was investigated. A PBPK model was developed
477 for the administration of Ambisome[®] to healthy subjects, which was used to identify the critical
478 factors for AmB release from liposomes and the *in vivo* predictability of the *in vitro* release
479 tests. The presence of BSA in the media was the most critical factor affecting the AmB release,
480 and the *in vitro* release profiles from tests with BSA in the medium were biopredictive.
481 Successful predictions of the “liposomal AmB” and the “released AmB” plasma concentration
482 profile were obtained with both hydrodynamic setups tested (sample and separate method and
483 continuous flow method). A PBPK-PD model of the activity of AmB on fungal cells was
484 developed based on the predicted "released AmB" plasma concentration profile in a
485 hypoalbuminaemic population in order to illustrate the potential of linking *in vitro* release
486 testing, PBPK modeling and microbiology data.

487

488 **Acknowledgments**

489 Part of this work has been previously presented at the AAPS PharmSci 360 annual meeting in
490 Washington, DC November 2018 (poster presentation). The authors would like to thank the
491 Mexican Council of Science and Technology (CONACyT) for the PhD scholarship of Dr R
492 Diaz de Leon-Ortega, Dr Wei-Feng Xue (University of Kent, UK) for his help with the AFM
493 studies, Dr Albert Bolhuis for his help with the microbiology studies and Dr Andrea Edginton
494 (University of Waterloo, Canada) for her help with PK-Sim[®] software.

495

496 **5. References**

- 497 [1] A. Abend, T. Heimbach, M. Cohen, F. Kesisoglou, X. Pepin, S. Suarez-Sharp, Dissolution
498 and Translational Modeling Strategies Enabling Patient-Centric Drug Product Development:
499 the M-CERSI Workshop Summary Report, *The AAPS Journal*, 20 (2018) 60.
- 500 [2] P. Espié, D. Tytgat, M.-L. Sargentini-Maier, I. Poggesi, J.-B. Watelet, Physiologically
501 based pharmacokinetics (PBPK), *Drug Metabolism Reviews*, 41 (2009) 391-407.
- 502 [3] F. Khalil, S. Laer, Physiologically based pharmacokinetic modeling: methodology,
503 applications, and limitations with a focus on its role in pediatric drug development, *Journal of*
504 *biomedicine & biotechnology*, 2011 (2011) 907461.
- 505 [4] H.M. Jones, I.B. Gardner, K.J. Watson, Modelling and PBPK Simulation in Drug
506 Discovery, *The AAPS Journal*, 11 (2009) 155-166.
- 507 [5] H.K. Batchelor, N. Fotaki, S. Klein, Paediatric oral biopharmaceutics: key considerations
508 and current challenges, *Advanced drug delivery reviews*, 73 (2014) 102-126.
- 509 [6] F. Kesisoglou, J. Chung, J. van Asperen, T. Heimbach, Physiologically Based Absorption
510 Modeling to Impact Biopharmaceutics and Formulation Strategies in Drug Development-
511 Industry Case Studies, *Journal of pharmaceutical sciences*, 105 (2016) 2723-2734.
- 512 [7] X. Zhuang, C. Lu, PBPK modeling and simulation in drug research and development, *Acta*
513 *Pharmaceutica Sinica B*, 6 (2016) 430-440.
- 514 [8] FDA, 2018. Physiologically Based Pharmacokinetic Analyses — Format and Content.
515 Available from:
516 <https://www.fda.gov/downloads/Drugs/GuidanceComplianceRegulatoryInformation/Guidances/UCM531207.pdf>. Access date: 31/07/2019.
- 517
518 [9] EMA, Guideline on the qualification and reporting of physiologically based
519 pharmacokinetic (PBPK) modelling and simulation, 2016. Available from:
520 <https://www.ema.europa.eu/documents/scientific-guideline/guideline-qualification-reporting->

521 physiologically-based-pharmacokinetic-pbpbk-modelling-simulation_en.pdf. Access date:
522 31/07/2019.

523 [10] X.Y. Zhang, M.N. Trame, L.J. Lesko, S. Schmidt, Sobol Sensitivity Analysis: A Tool to
524 Guide the Development and Evaluation of Systems Pharmacology Models, CPT:
525 pharmacometrics & systems pharmacology, 4 (2015) 69-79.

526 [11] K. McNally, R. Cotton, G.D. Loizou, A Workflow for Global Sensitivity Analysis of
527 PBPK Models, Frontiers in pharmacology, 2 (2011) 31.

528 [12] M. Ulldemolins, J.A. Roberts, J. Rello, D.L. Paterson, J. Lipman, The effects of
529 hypoalbuminaemia on optimizing antibacterial dosing in critically ill patients, Clinical
530 Pharmacokinetics, 50 (2011) 99-110.

531 [13] L. Kuepfer, C. Niederalt, T. Wendl, J.F. Schlender, S. Willmann, J. Lippert, M. Block, T.
532 Eissing, D. Teutonico, Applied Concepts in PBPK Modeling: How to Build a PBPK/PD Model,
533 CPT: pharmacometrics & systems pharmacology, 5 (2016) 516-531.

534 [14] K. Chen, S. Teo, K.Y. Seng, Sensitivity analysis on a physiologically-based
535 pharmacokinetic and pharmacodynamic model for diisopropylfluorophosphate-induced
536 toxicity in mice and rats, Toxicology mechanisms and methods, 19 (2009) 486-497.

537 [15] E. Asin-Prieto, A. Rodriguez-Gascon, A. Isla, Applications of the
538 pharmacokinetic/pharmacodynamic (PK/PD) analysis of antimicrobial agents, Journal of
539 infection and chemotherapy : official journal of the Japan Society of Chemotherapy, 21 (2015)
540 319-329.

541 [16] E.I. Nielsen, O. Cars, L.E. Friberg, Pharmacokinetic/pharmacodynamic (PK/PD) indices
542 of antibiotics predicted by a semimechanistic PKPD model: a step toward model-based dose
543 optimization, Antimicrobial agents and chemotherapy, 55 (2011) 4619-4630.

544 [17] M.W. Sadiq, E.I. Nielsen, D. Khachman, J.M. Conil, B. Georges, G. Houin, C.M. Laffont,
545 M.O. Karlsson, L.E. Friberg, A whole-body physiologically based pharmacokinetic (WB-

546 PBPK) model of ciprofloxacin: a step towards predicting bacterial killing at sites of infection,
547 *Journal of pharmacokinetics and pharmacodynamics*, 44 (2017) 69-79.

548 [18] J. Mora-Duarte, R. Betts, C. Rotstein, A.L. Colombo, L. Thompson-Moya, J. Smietana,
549 R. Lupinacci, C. Sable, N. Kartsonis, J. Perfect, Comparison of caspofungin and amphotericin
550 B for invasive candidiasis, *The New England journal of medicine*, 347 (2002) 2020-2029.

551 [19] E.M. Johnson, J.O. Ojwang, A. Szekely, T.L. Wallace, D.W. Warnock, Comparison of In
552 Vitro Antifungal Activities of Free and Liposome-Encapsulated Nystatin with Those of Four
553 Amphotericin B Formulations, *Antimicrob. Agents. Chemother.*, 42 (1998) 1412-1416.

554 [20] L. Kagan, P. Gershkovich, K.M. Wasan, D.E. Mager, Physiologically Based
555 Pharmacokinetic Model of Amphotericin B Disposition in Rats Following Administration of
556 Deoxycholate Formulation (Fungizone®): Pooled Analysis of Published Data, *The AAPS*
557 *Journal*, 13 (2011) 255.

558 [21] L. Kagan, P. Gershkovich, K.M. Wasan, D.E. Mager, Dual Physiologically Based
559 Pharmacokinetic Model of Liposomal and Nonliposomal Amphotericin B Disposition,
560 *Pharmaceutical Research*, 31 (2014) 35-45.

561 [22] R. Díaz de León–Ortega, D.M. D'Arcy, N. Fotaki, Investigating Factors That Affect In
562 vitro Drug Release From A Parenteral Liposomal Formulation, in: *AAPS*, Washington DC,
563 USA, 2018.

564 [23] R. Diaz de Leon-Ortega, D.M. D'Arcy, D.L. Lamprou, W.F. Xue, N. Fotaki, In vitro in
565 vivo relations for the parenteral liposomal formulation of Amphotericin B. Part 1: A
566 biorelevant and clinically relevant approach, Submitted to the *Journal of Controlled Release*,
567 (2019).

568 [24] P. Egger, R. Bellmann, C.J. Wiedermann, Determination of amphotericin B, liposomal
569 amphotericin B, and amphotericin B colloidal dispersion in plasma by high-performance liquid
570 chromatography, *J. Chromatogr. B: Anal. Technol. Biomed. Life Sci.*, 760 (2001) 307-313.

571 [25] R. Diaz de Leon-Ortega, D.M. D'Arcy, A. Bolhuis, N. Fotaki, Investigation and simulation
572 of dissolution with concurrent degradation under healthy and hypoalbuminaemic simulated
573 parenteral conditions- case example Amphotericin B, European journal of pharmaceutics and
574 biopharmaceutics : official journal of Arbeitsgemeinschaft fur Pharmazeutische
575 Verfahrenstechnik e.V, (2018).

576 [26] N. Fotaki, Flow-through cell apparatus (USP apparatus 4): Operation and features,
577 Dissolution Technol, 18 (2011) 46-49.

578 [27] I. Bekersky, R.M. Fielding, D.E. Dressler, J.W. Lee, D.N. Buell, T.J. Walsh,
579 Pharmacokinetics, Excretion, and Mass Balance of Liposomal Amphotericin B (AmBisome)
580 and Amphotericin B Deoxycholate in Humans, Antimicrobial Agents and Chemotherapy, 46
581 (2002) 828-833.

582 [28] I. Bekersky, R.M. Fielding, D.E. Dressler, J.W. Lee, D.N. Buell, T.J. Walsh, Plasma
583 protein binding of amphotericin B and pharmacokinetics of bound versus unbound
584 amphotericin B after administration of intravenous liposomal amphotericin B (AmBisome) and
585 amphotericin B deoxycholate, Antimicrob. Agents. Chemother., 46 (2002) 834-840.

586 [29] DrugBank, Amphotericin B, 2005. Available from:
587 <https://www.drugbank.ca/drugs/DB00681>. Access date: 31/07/2019

588 [30] Sigma-Aldrich, Amphotericin B, 2015. Available from:
589 [https://www.sigmaaldrich.com/content/dam/sigma-](https://www.sigmaaldrich.com/content/dam/sigma-aldrich/docs/Sigma/Datasheet/6/a9528dat.pdf)
590 [aldrich/docs/Sigma/Datasheet/6/a9528dat.pdf](https://www.sigmaaldrich.com/content/dam/sigma-aldrich/docs/Sigma/Datasheet/6/a9528dat.pdf). Access date: 31/07/2019

591 [31] S.S. Bharate, V. Kumar, R.A. Vishwakarma, Determining Partition Coefficient (Log P),
592 Distribution Coefficient (Log D) and Ionization Constant (pKa) in Early Drug Discovery,
593 Combinatorial chemistry & high throughput screening, 19 (2016) 461-469.

594 [32] ChemSpider, Amphotericin B, 2015. Available from:
595 <http://www.chemspider.com/Chemical-Structure.10237579.html>. Access date: 31/07/2019

596 [33] M.T. Lamy-Freund, V.F. Ferreira, S. Schreier, Polydispersity of aggregates formed by the
597 polyene antibiotic amphotericin B and deoxycholate. A spin label study, *Biochim. Biophys.*
598 *Acta, Biomembr.*, 981 (1989) 207-212.

599 [34] J. Mazerski, J. Grzybowska, E. Borowski, Influence of net charge on the aggregation and
600 solubility behaviour of amphotericin B and its derivatives in aqueous media, *European*
601 *biophysics journal*, 18 (1990) 159-164.

602 [35] J. Barwicz, S. Christian, I. Gruda, Effects of the aggregation state of amphotericin B on
603 its toxicity to mice, *Antimicrob. Agents. Chemother.*, 36 (1992) 2310-2315.

604 [36] Y. Ridente, J. Aubard, J. Bolard, Absence in amphotericin B-spiked human plasma of the
605 free monomeric drug, as detected by SERS, *FEBS letters*, 446 (1999) 283-286.

606 [37] Gilead, Ambisome®,
607 [http://www.gilead.com/~~/media/files/pdfs/medicines/other/ambisome/ambisome_pi.pdf?la=e](http://www.gilead.com/~~/media/files/pdfs/medicines/other/ambisome/ambisome_pi.pdf?la=en)
608 [n](http://www.gilead.com/~~/media/files/pdfs/medicines/other/ambisome/ambisome_pi.pdf?la=en), (2015).

609 [38] Y. Yokouchi, T. Tsunoda, T. Imura, H. Yamauchi, S. Yokoyama, H. Sakai, M. Abe, Effect
610 of adsorption of bovine serum albumin on liposomal membrane characteristics, *Colloids and*
611 *Surfaces B: Biointerfaces*, 20 (2001) 95-103.

612 [39] T. Hernández-Caselles, J. Villalaín, J.C. Gómez-Fernández, Influence of liposome charge
613 and composition on their interaction with human blood serum proteins, *Molecular and Cellular*
614 *Biochemistry*, 120 (1993) 119-126.

615 [40] S.L. Law, W.Y. Lo, S.H. Pai, G.W. Teh, F.Y. Kou, The adsorption of bovine serum
616 albumin by liposomes, *International Journal of Pharmaceutics*, 32 (1986) 237-241.

617 [41] B. Misme-Aucouturier, M. Albassier, N. Alvarez-Rueda, P. Le Pape, Specific Human and
618 *Candida Cellular Interactions Lead to Controlled or Persistent Infection Outcomes during*
619 *Granuloma-Like Formation*, *Infection and Immunity*, 85 (2017) e00807-00816.

620 [42] C.D. Pfeiffer, G.P. Samsa, W.A. Schell, L.B. Reller, J.R. Perfect, B.D. Alexander,
621 Quantitation of Candida CFU in Initial Positive Blood Cultures, Journal of Clinical
622 Microbiology, 49 (2011) 2879-2883.

623

624 **Tables**

625 **Table 1.** Levels and factors investigated with the sample and separate setup for the release
626 studies of AmB from Ambisome® in clinically relevant media.

Level	BSA %w/v	Medium	Agitation (rpm)
- 1	2.0	PBS BS 19.8 mM PL 7.9 mM	130 (Low Agitation)
+ 1	4.0	KRB BS 20.0 mM PL 4.0 mM	380 (High Agitation)

627

Table 2. PK-Sim model set up: physicochemical properties, distribution and clearance parameters of "released AmB" and "liposomal AmB" (Ambisome[®]) after administration to healthy subjects.

"Released AmB"	
Molecular weight (g/mol)	924 [29, 30]
log P	0.80 [29], 0.94 [31], 1.84 [31], 2.14 [31]
clog P	- 2.33 [29], - 0.66 [29], 1.16 [32]
pka	acidic 5.5 [30], basic 10.0 [30]
Solubility at pH = 7	0.09 µg/mL [33], 1.38 µg/mL [34], 6.00 µg/mL [35]
fraction unbound (albumin)	0.05 [28]
Distribution volume	2340 ± 202 mL/kg [27]
Cl_{renal}	0.07 ± 0.01 mL/min/kg [27]. GFR fraction = 0.875
Cl_{biliary}	0.09 ± 0.02 mL/min/kg [27]. k _{bil} = 0.002 h ⁻¹

Binding partners	alfa 1 acid glycoprotein (AAG1), EST expression, $k_{\text{diss}} = 1.07 - 2.44 \mu\text{mol/L}$ (approximation from unbound fraction) [27]
	beta lipoprotein (APOB), EST expression, $k_{\text{diss}} = 0.25 \mu\text{mol/L}$ [36]
"Liposomal AmB"	
Distribution volume	$1628 \pm 876 \text{ mL/kg}$ [27]
Cl renal	$0.01 \pm 0.00 \text{ mL/min/kg}$ [27], GFR fraction = 0.125
Cl biliary	$0.01 \pm 0.00 \text{ mL/min/kg}$ [27], $k_{\text{bil}} = 0.0003 \text{ h}^{-1}$
Assumptions for the model, considering the "liposomal AmB" as a molecule	
Molecular weight (g/mol)	924
Radius (solute)	80 nm [37]
log P	Parameter to identify, starting value 0.8
pka	Neutral

Solubility at pH = 7	290 mg/mL [calculated from the total amount of powder in a formulation vial (14.5 g), dissolved in 50 mL of water]								
fraction unbound albumin	0.05								
Immune removal	<p>Metabolizing enzymes -> Intrinsic clearance First order -></p> <p>Relative expression -> Intracellular -> Endosomal</p> <table> <tr> <td>Plasma</td> <td>100%</td> </tr> <tr> <td>Liver periportal</td> <td>100%</td> </tr> <tr> <td>Liver pericentral</td> <td>100%</td> </tr> <tr> <td>Spleen</td> <td>100%</td> </tr> </table>	Plasma	100%	Liver periportal	100%	Liver pericentral	100%	Spleen	100%
Plasma	100%								
Liver periportal	100%								
Liver pericentral	100%								
Spleen	100%								

Table 3. Parameters and the range in which the parameters were investigated in the sensitivity analysis of the validated PBPK model of Ambisome[®] administration.

Parameter	Abbreviation	Interval tested
log P ("liposomal AmB")	logP (lip)	0 – 2 (log units)
log P ("released AmB")	logP (rel)	2.24 – 4.24 (log units)
Aqueous solubility ("liposomal AmB")	Sol (lip)	90 – 490 (µg/mL)
Aqueous solubility ("released AmB")	Sol (rel)	0.01 – 6.00 (µg/mL)
Radius solute ("liposomal AmB")	Rad (lip)	40 – 120 (nm)
k_{bil} ("liposomal AmB")	Bil (lip)	0.0001 – 0.0005 (h ⁻¹)
k_{bil} ("released AmB")	Bil (rel)	0.001 – 0.003 (h ⁻¹)
GFR ("liposomal AmB")	GFR (lip)	0 – 1 (fraction)
GFR ("released AmB")	GFR (rel)	0 – 1 (fraction)
"Immune enzyme" specific clearance	Imm	1.57 – 3.57 (h ⁻¹)
APOB1 k_{diss}	APOB1	0.12 – 0.37 (µmol/L)
AAG1 k_{diss}	AAG1	0.21 – 0.63 (µmol/L)
k_{rel-iv}	krel	0.114 - 3.539 (h ⁻¹)
Unbound fraction ("liposomal AmB")	fU (lip)	0.05 – 0.95 (fraction)

Unbound fraction ("released AmB")	fU (rel)	0.05 – 0.95 (fraction)
-----------------------------------	----------	------------------------

Table 4. Parameters obtained after fitting (Eq 3) of %AmB released profiles from Ambisome® with the sample and separate setup and the continuous flow setup [LA: low agitation, HA: high agitation, LV: low velocity, HV: high velocity] (Mean ± SD, n = 3).

Buffer	BSA (%w/v)	Surfactant concentrations	Agitation/velocity	k_{rel} (h ⁻¹)	%AmB _{releasedmax}
Sample and separate					
PBS	0.0	BS 19.8 mM PL 7.9 mM	LA	1.425 ± 0.101	96.258 ± 0.101
PBS	4.0	BS 19.8 mM PL 7.9 mM	LA	0.701 ± 0.060	78.573 ± 2.548
KRB	0.0	BS 20.0 mM PL 4.0 mM	LA	3.034 ± 0.106	99.201 ± 0.321
KRB	4.0	BS 20.0 mM PL 4.0 mM	LA	0.621 ± 0.192	81.662 ± 2.931
PBS	0.0	BS 19.8 mM PL 7.9 mM	HA	2.437 ± 0.129	98.953 ± 0.158
PBS	4.0	BS 19.8 mM PL 7.9 mM	HA	0.410 ± 0.052	73.031 ± 6.013
KRB	0.0	BS 20.0 mM PL 4.0 mM	HA	2.747 ± 0.046	99.146 ± 0.072

KRB	4.0	BS 20.0 mM PL 4.0 mM	HA	0.896 ± 0.041	88.141 ± 2.480
Continuous flow					
KRB	0.0	BS 20.0 mM PL 4.0 mM	LV	0.305 ± 0.071	49.181 ± 17.119
KRB	4.0	BS 20.0 mM PL 4.0 mM	LV	0.467 ± 0.162	43.101 ± 10.563
KRB	0.0	BS 20.0 mM PL 4.0 mM	HV	1.364 ± 1.890	60.416 ± 4.593
KRB	4.0	BS 20.0 mM PL 4.0 mM	HV	-	-

Table 5. Properties of liposomes obtained from atomic force microscopy from the samples prepared in media with BS PL in the presence and absence of BSA. Mean \pm SD. n = 20 Random Particles.

Sample	Diameter (nm)	Surface Roughness (nm)	Density (μm^{-2})
KRB control (centrifugation/vacuum)	69.4 \pm 18.9	12.9 \pm 1.6	11.9
KRB BS 20.0 mM PL 4.0 mM	130.0 \pm 13.0	10.1 \pm 2.7	7.7
KRB BS 20.0 mM PL 4.0 mM BSA 4.0% w/v	No Particles		

Table 6. Parameters obtained after fitting (Equation 6) of CFU time profiles from time killing experiments in KRB BSA 2 and 4% w/v using different concentrations of AmB (0.75, 1.5 and 3.0 $\mu\text{g}/\text{mL}$) (Mean \pm SD, n = 2).

BSA (%w/v)	AmB ($\mu\text{g}/\text{mL}$)	%CFU _{max}	k_{kill} (h^{-1})	R ²	AIC
2.0	0.75	105.1 \pm 5.23	0.33 \pm 0.03	0.86 \pm 0.02	52.88 \pm 0.3
	1.50	110.65 \pm 4.17	0.54 \pm 0.03	0.93 \pm 0.05	47.16 \pm 6.17
	3.00	110.6 \pm 5.37	0.77 \pm 0.11	0.92 \pm 0.05	48 \pm 6.43
4.0	0.75	101.75 \pm 4.6	0.11 \pm 0.01	0.89 \pm 0.01	47.25 \pm 2.38
	1.50	123.8 \pm 10.04	0.17 \pm 0.03	0.84 \pm 0.07	54.71 \pm 5.18
	3.00	107.65 \pm 6.15	0.37 \pm 0.01	0.9 \pm 0	50.27 \pm 1.06

Figure captions

Figure 1. Workflow for the PBPK modeling of "liposomal AmB" and "released AmB" after the administration of Ambisome[®] to healthy subjects

Figure 2. Workflow for the PBPK-PD modeling of the liposomal and released AmB after the administration of Ambisome[®] to a hypoalbuminaemic population in order to simulate the pharmacological activity of the released AmB on *C. albicans*.

Figure 3. % AmB released with the a) sample and separate and the b) continuous flow setup at 37 °C to investigate the effect of the type of buffer, the BSA 4.0% w/v presence and the hydrodynamics in clinically relevant media with BS – PL. (Mean ± SD, n=3; solid lines: media with BSA 4.0% w/v; dotted lines: media without BSA 4.0% w/v).

Figure 4. Pareto charts for the estimated effects of the main factors and 2 level interactions of the analysis of a) % $AmB_{releasedmax}$ and k_{rel} from the sample and separate setup and b) the AUC_{0-12h} from the continuous flow method. A factor was significant when the estimated effect (horizontal bars) was larger than the standardized effect (vertical line).

Figure 5. AFM images to evaluate the effect of media components on Ambisome[®] liposomes. a) KRB BS 20.0 mM PL 4.0 mM, b) KRB BS 20.0 mM PL 4.0 mM BSA 4.0% w/v. The scale bar represents 200 nm.

Figure 6. Observed and simulated (PBPK model) plasma concentration profiles of "liposomal AmB" and "released AmB" after the administration of Ambisome[®] to healthy subjects [25, 26].

Figure 7. Sensitivity analysis of PBPK model parameters on the "liposomal AmB" and "released AmB" AUC_{0-24h} obtained from simulated plasma concentrations in healthy subjects. The black line is the AUC_{0-24h} obtained from the validated PBPK model for healthy subjects.

Figure 8. AUC_{0-24h} calculated from simulated plasma concentration profiles with with the k_{rel} from the *in vitro* release profiles against the AUC_{0-24h} obtained from the validated PBPK model for "liposomal AmB" and "released AmB". n = 5 subjects for each population.

Figure 9. PBPK-PD model for a hypoalbuminaemic population (plasma protein fraction 0.5; healthy subjects: plasma protein fraction 1.0) –Simulated concentration and its pharmacodynamic effect on fungal cells. a) Simulated plasma concentration profiles of "liposomal AmB" and "released AmB" from the validated PBPK model for healthy subjects and the hypothesised model for the hypoalbuminaemic population, b) simulation of plasma concentrations following administration of a 300 mg dose of Ambisome[®], c) simulated time killing rate coefficient (k_{kill}) (corresponding to the simulated plasma concentration profile of Figure 9b), and d) effect of the administration of Ambisome[®] on the growth of *Candida albicans*.

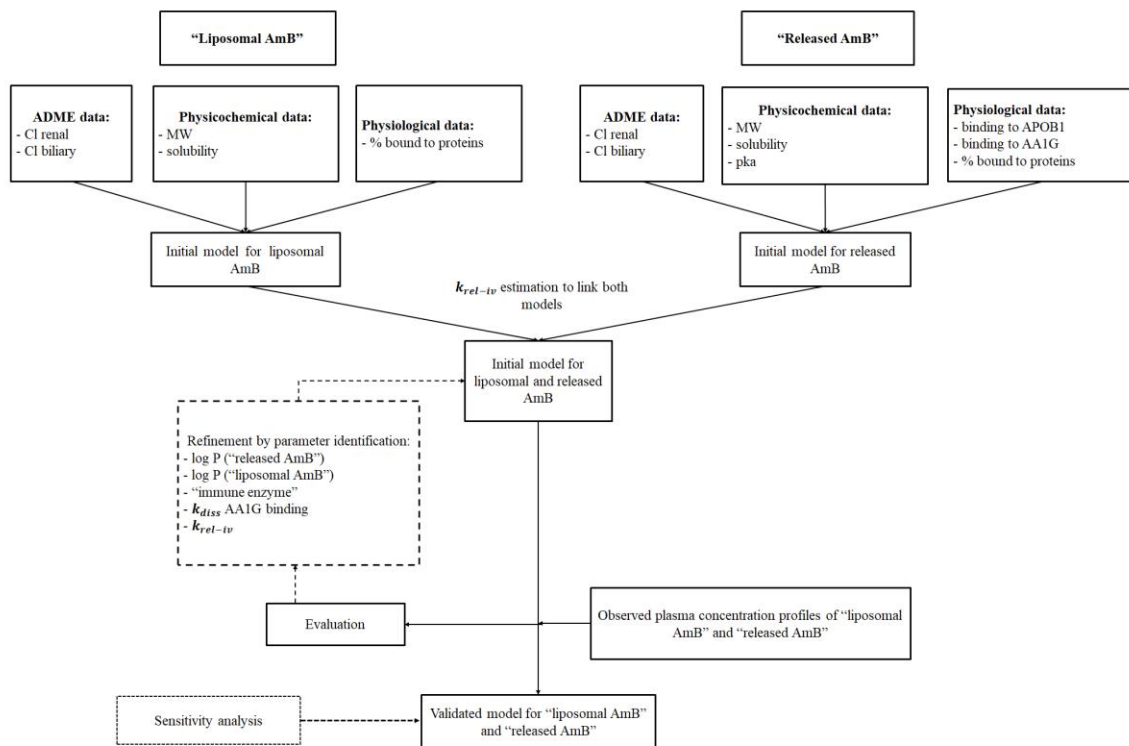


Figure 1

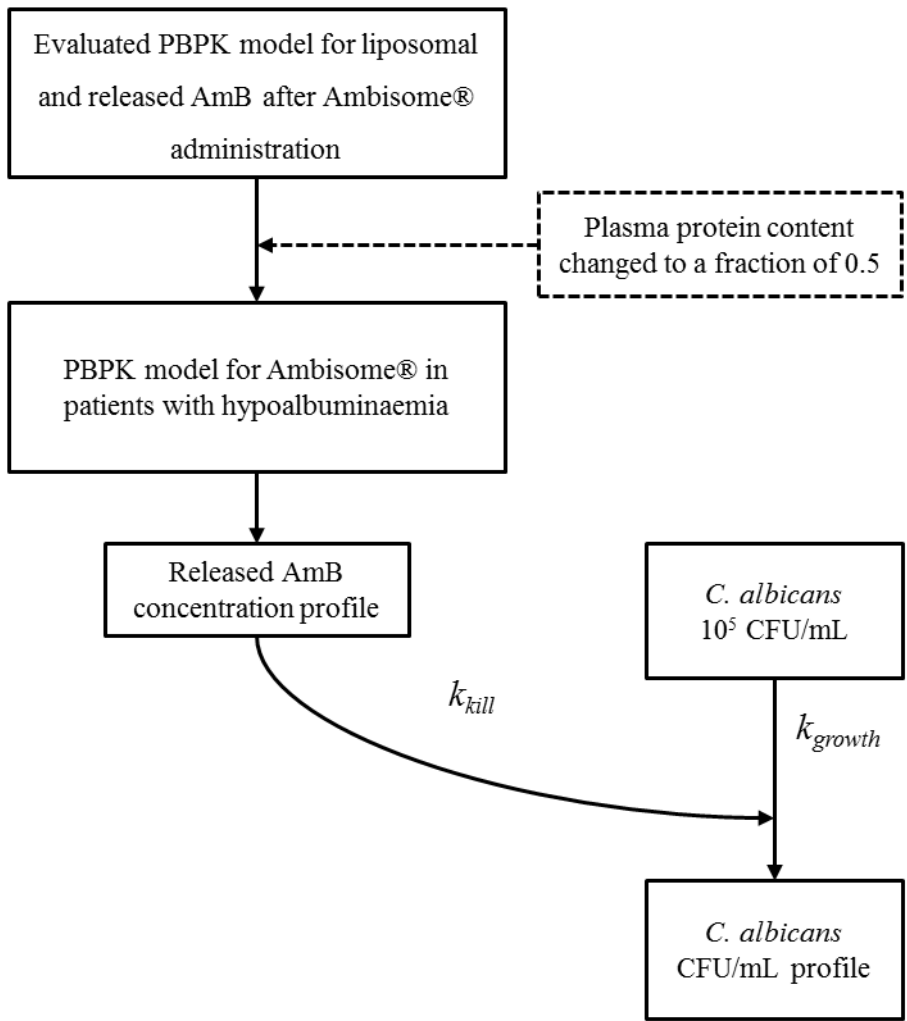


Figure 2

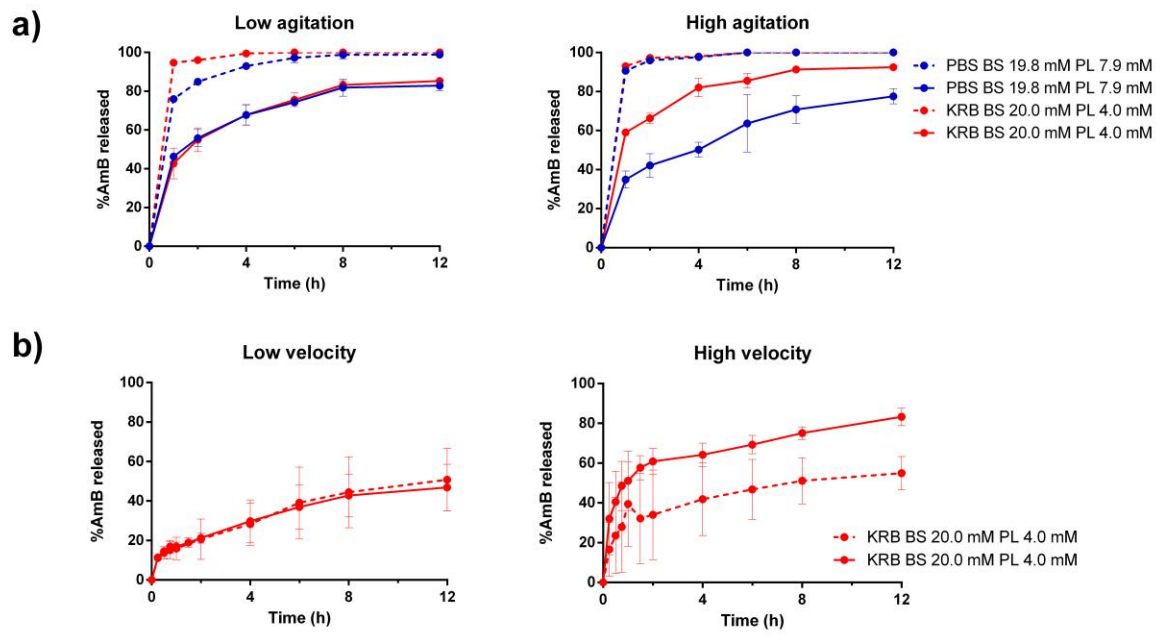


Figure 3

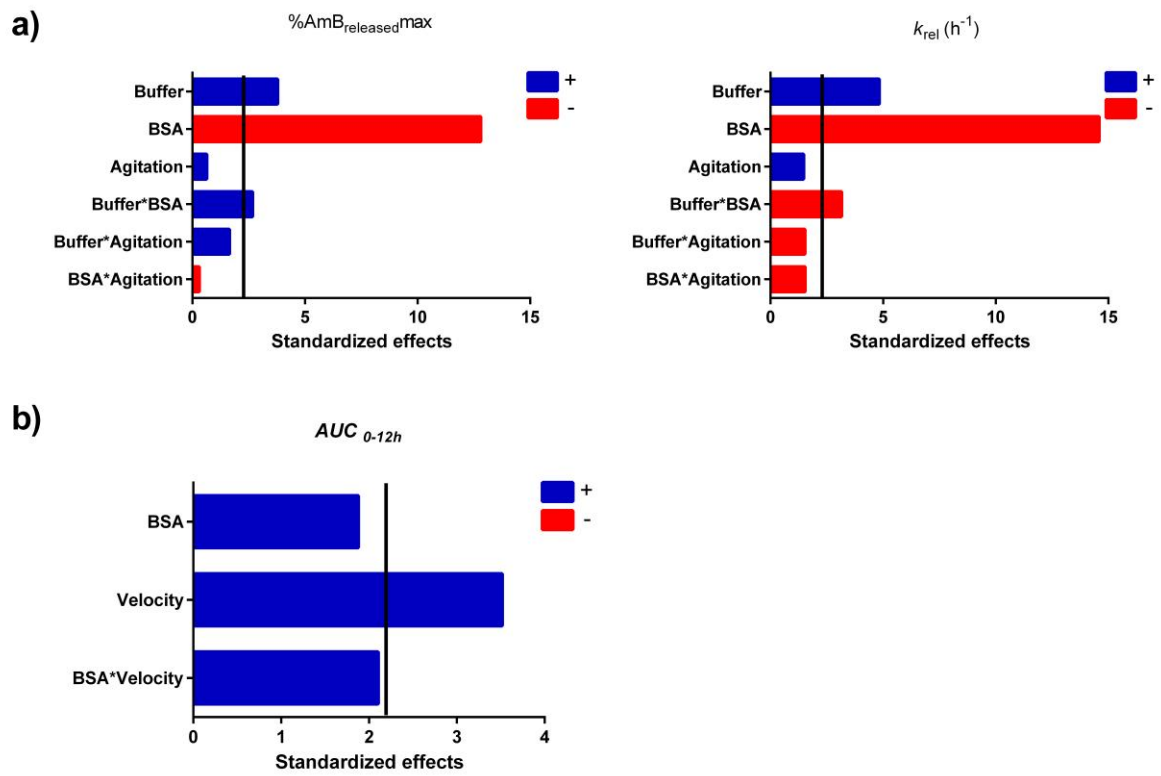


Figure 4

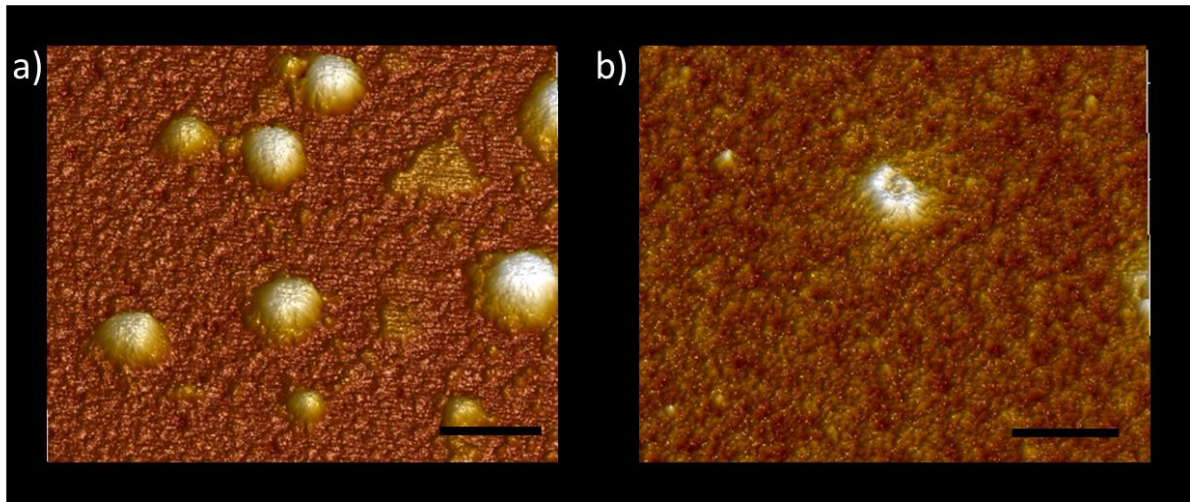


Figure 5

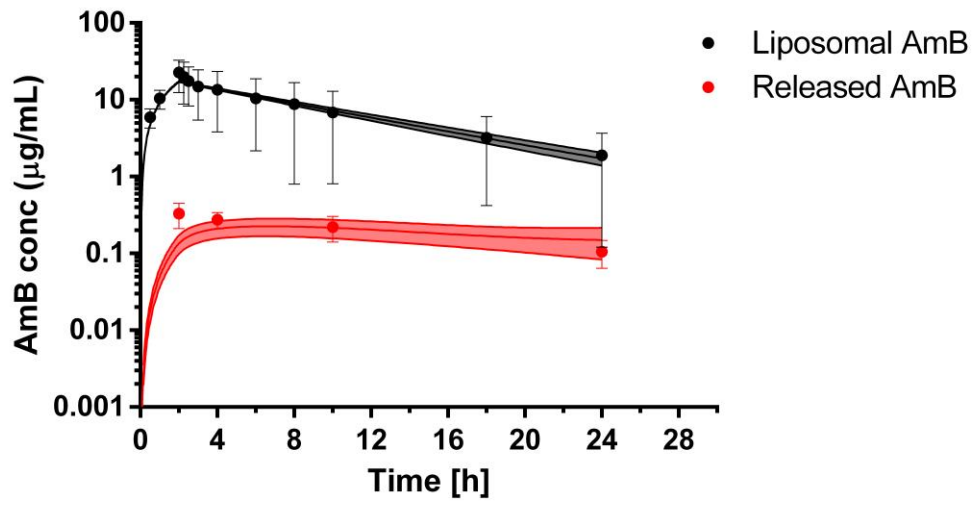


Figure 6

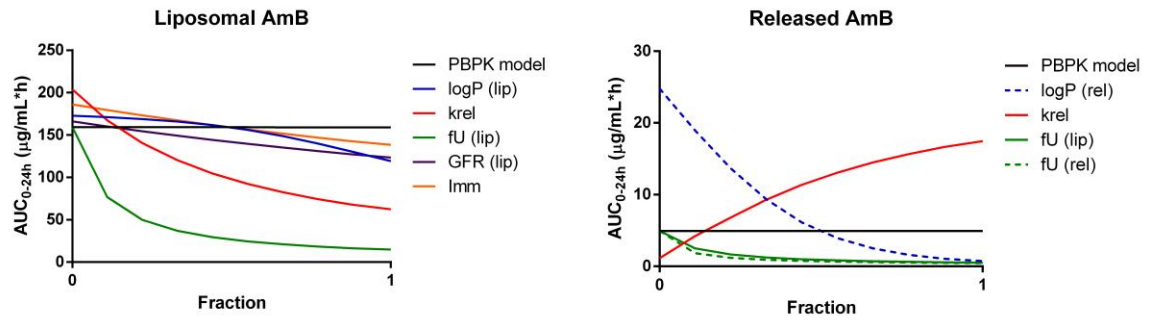


Figure 7

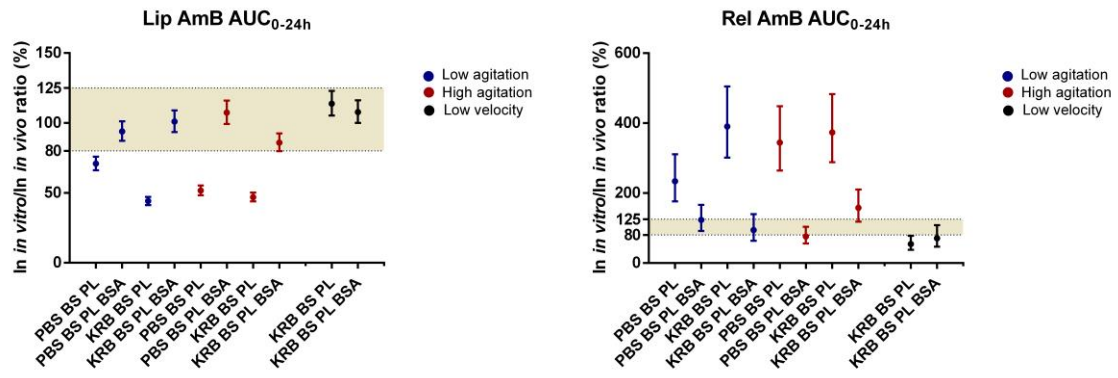


Figure 8

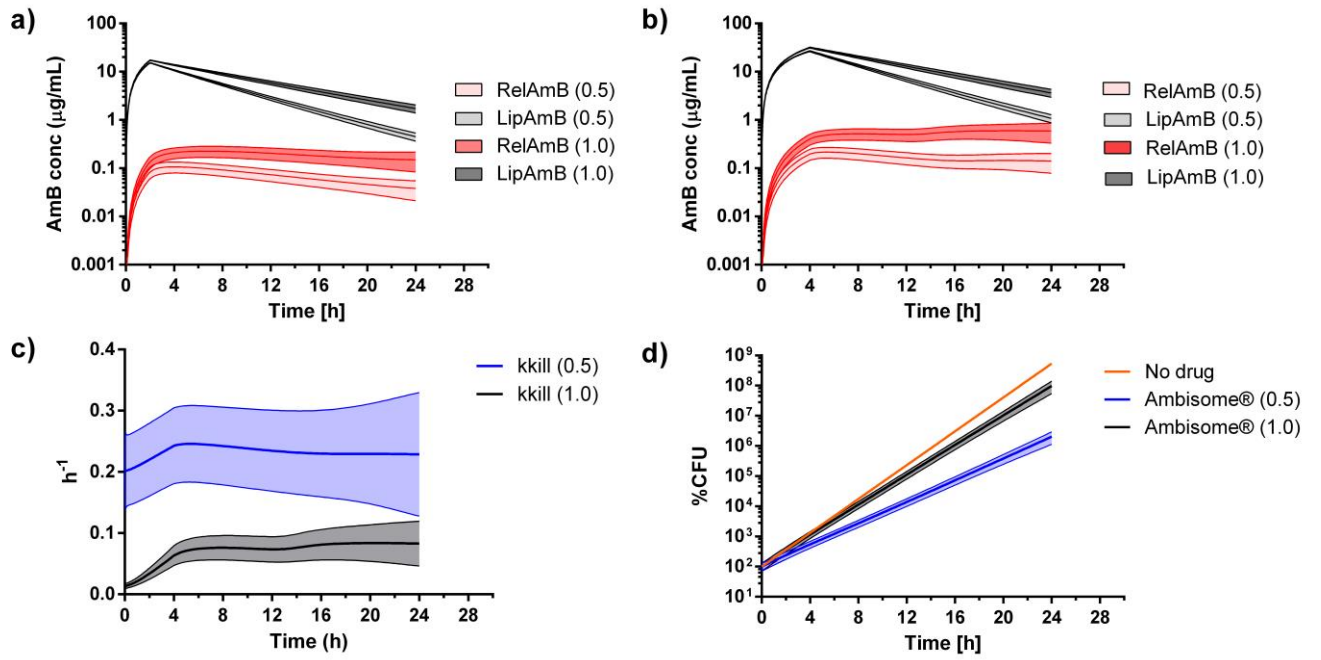


Figure 9